

## Ten-year climatology of potassium number density at 54° N, 12° E



J. Lautenbach <sup>a,\*</sup>, J. Höffner <sup>b</sup>, F.-J. Lübken <sup>b</sup>, M. Kopp <sup>b</sup>, M. Gerding <sup>b</sup>

<sup>a</sup> Arecibo Observatory, SRI International, HC-3 Box 53995, Arecibo, PR 00612, USA

<sup>b</sup> Leibniz Institute of Atmospheric Physics, Schloss-Str. 6, 18225 Kühlungsborn, Germany

### ARTICLE INFO

#### Article history:

Received 24 May 2016

Received in revised form

18 May 2017

Accepted 20 June 2017

Available online 23 June 2017

#### Keywords:

Resonance Doppler lidar

Observation

Potassium layer

Mesosphere and lower thermosphere

### ABSTRACT

In the years from 2002 to 2012 potassium densities observations were performed in the mesopause region at Kühlungsborn using a potassium Doppler lidar. The 10-year diurnal data set comprises 5090 h of potassium number densities at 741 days with 25.2% under full daylight conditions. Potassium number densities show a clear semi-annual variation with two broad maxima reoccurring every year. The first maximum occurs in summer and lasts for about 4 months (May–August) with number densities up to 60 atoms/cc. The second maximum is observed from early December to late February with densities up to 30 atoms/cc. Both the peak density and the column density are higher at solstices than at equinoxes. The large data set shows little variation of the mean layer over the 10 years.

© 2017 The Authors. Published by Elsevier Ltd. This is an open access article under the CC BY license (<http://creativecommons.org/licenses/by/4.0/>).

## 1. Introduction

The existence and properties of metal layers in the mesosphere lower thermosphere (MLT) region (80–110 km) has been of great interest for decades. It is generally assumed that the ablation of meteoroids is the only source for metal species observed in the mesopause region whereas sinks are given by chemistry and transport. It was [Slipher \(1929\)](#) who recorded the first detection of sodium airglow in the mesopause region by the use of optical instruments. Later [Sullivan and Hunten \(1962\)](#) observed the first airglow emission of potassium D<sub>1</sub>. The first lidar observations of potassium D<sub>1</sub> were obtained by [Felix et al. \(1973\)](#). Later [Höffner and von Zahn \(1995\)](#) and [Papen et al. \(1995\)](#) introduced potassium Doppler lidars. With their low error and high resolution, potassium Doppler lidars contribute significantly to our understanding of the potassium layer. Potassium observations were made at various locations like Spitsbergen (78° N), Kühlungsborn (54° N), Tenerife (28° N), Arecibo (18° N) and an ocean voyage from 45° N to 71° S ([Höffner and Lübken, 2007](#); [Eska et al., 1998](#); [Fricke-Begemann et al., 2002b](#); [Friedman et al., 2002](#); [Eska et al., 1999](#)). These observations established our current understanding of the seasonal behaviour of the potassium layer. However, most of the early data sets are based on short campaign-like measurements except for Kühlungsborn (54° N) and Arecibo (18° N) which have continuous measurements over many years. Furthermore, lidar

measurements in the past were limited to night times due to the high solar background at day time. Therefore little is known about the properties of metal layers from lidar observation at daytime.

In this paper we present and discuss a diurnal 10-year climatology of potassium densities in the MLT region (80–110 km) at Kühlungsborn (54° N). Potassium shows, in contrast to all other known metal species, a semi-annual variation. With the help of this data set the unusual behaviour of the potassium layer over Kühlungsborn was recently understood and finally explained by [Plane et al. \(2014\)](#). [Plane et al. \(2014\)](#) is concluding in his publication: "There are two factors involved. First, the K<sup>+</sup> ion is more difficult to neutralize because it can only form weakly bound cluster ions at very low temperatures. Thus, the low temperatures of the summertime MLT shift the balance from K<sup>+</sup> to K, accounting for the summertime maximum. The second factor concerns the neutral chemistry. None of the reactions involving KO, KO<sub>2</sub>, and KOH has a significant temperature dependence. In contrast, the activation energy for the reaction KHCO<sub>3</sub> + H is so large that this reaction never plays a significant role, even during the warmest period in winter. The only route from KHCO<sub>3</sub> back to K is via photolysis, and this is essentially temperature independent." The presented multi-year data set has been also essential for: a comprehensive tidal study from the stratosphere to the mesosphere by [Kopp et al. \(2015\)](#), the first explanation of the unusual behaviour of potassium by resolving the chemistry by [Plane et al. \(2014\)](#), the

\* Corresponding author.

E-mail address: [jens.lautenbach@sri.com](mailto:jens.lautenbach@sri.com) (J. Lautenbach).

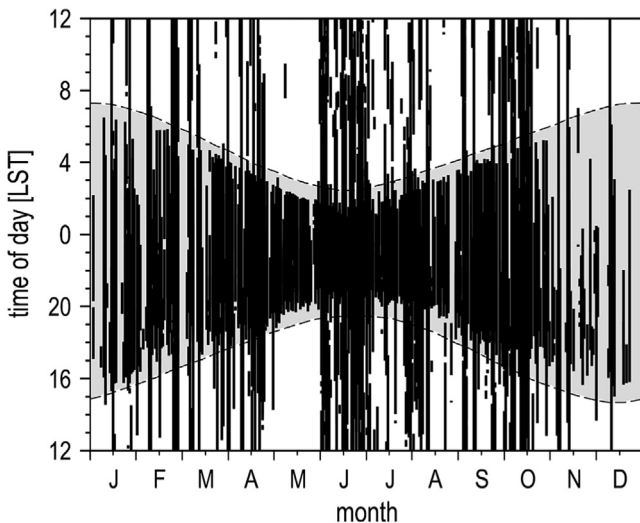


**Fig. 1.** Local time coverage of K-lidar observations at Kühlungsborn ( $54^{\circ}$  N) from February 2002 to February 2012.

development of a satellite retrieval method for potassium from OSIRIS (Optical Spectrograph and InfraRed Imager System (Llewellyn et al., 2004)) by Dawkins et al. (2014) and the validation of tides in the potassium layer for the WACCM-K model by Feng et al. (2015).

## 2. Instrumentation

The scanning potassium Doppler lidar (K-lidar) of the Leibniz-Institute of Atmospheric Physics in Kühlungsborn was primarily designed for temperature profiling in the MLT region (von Zahn and Höffner, 1996). By scanning the Doppler broadened potassium resonance line, potassium number densities as well as temperatures are obtained. We note that several effects are not important for the potassium lidar but are most likely relevant for resonance lidars based on other species such as sodium or iron. This includes the Hanle effect caused by the Earth's magnetic field, Zeeman and Stark effects, and absorption within the metal layer (Fricke and von Zahn, 1985; Alpers et al., 1990; von Zahn and Höffner, 1996). Resonance lidar measurements rely on accurate intensity measurements at different wavelengths. We use identical optical paths and counting electronics for each individual laser pulse to avoid

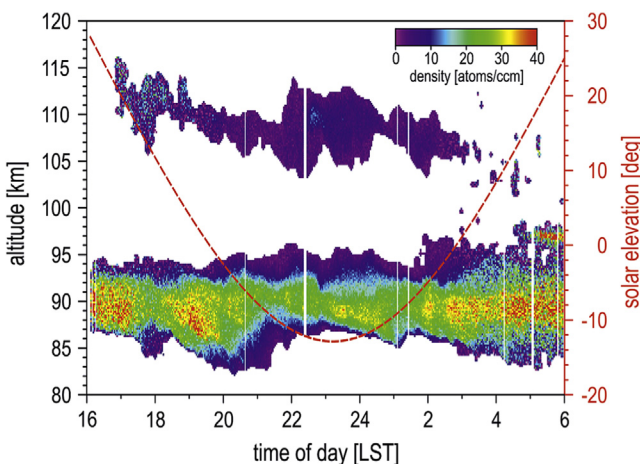


**Fig. 2.** Example of a measurement from June 10, 2011. Potassium number density (colour coded) and solar elevation (right axis). Densities are larger than 2 atoms/ccm on a 2 min time and 200 m altitude grid.

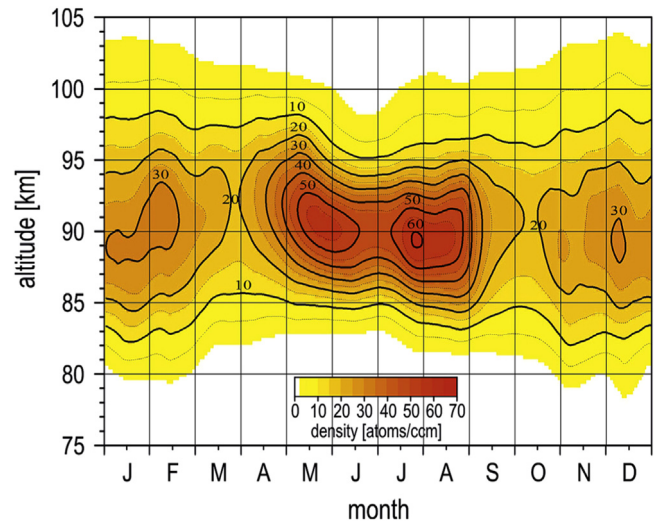


**Fig. 3.** Ten-year climatology of potassium density at  $54^{\circ}$  N. The data were smoothed using a 21 day Hanning filter. Densities lower than 2 atoms/ccm are not shown.

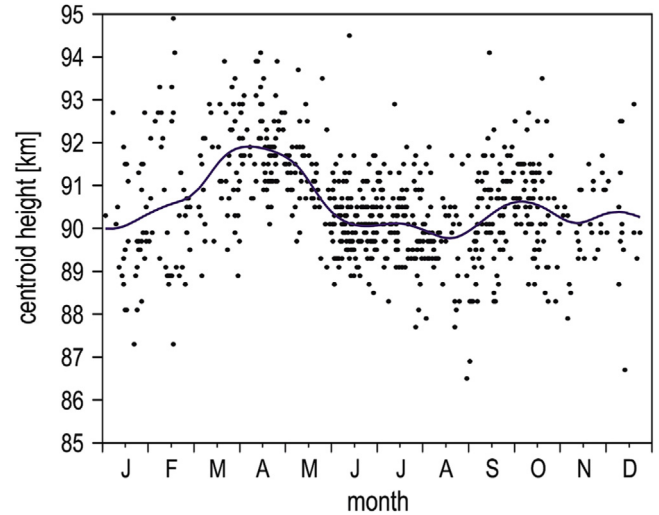


**Fig. 4.** Centroid height of the ten-year potassium data set at  $54^{\circ}$  N. The data were smoothed using a 21 day Hanning filter.

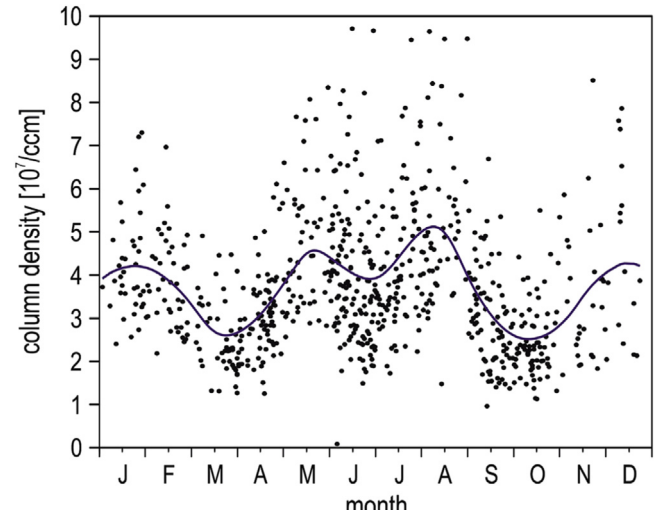


**Fig. 5.** Column density of the ten-year potassium data set at  $54^{\circ}$  N. The data were smoothed using a 21 day Hanning filter.

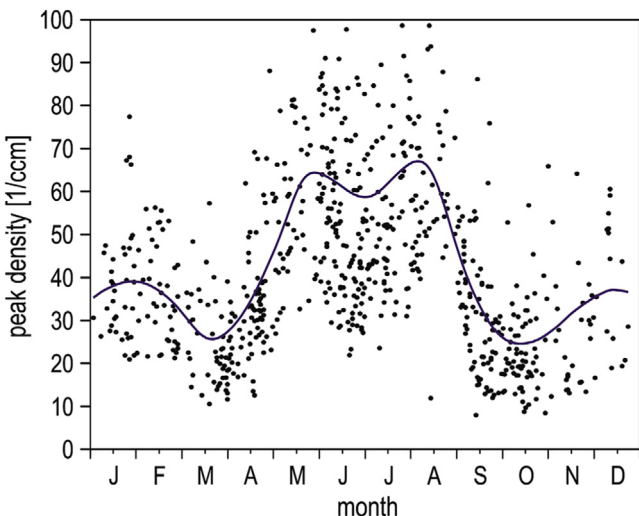


**Fig. 6.** Peak number density of the ten-year potassium data set at  $54^\circ$  N. The data were smoothed using a 21 day Hanning filter.

any bias caused by performance differences. In addition, a complete spectral scan of the resonance line takes less than 1 s which eliminates the effects of natural variability in tropospheric transmission and K atom number densities. The mobile K-lidar of the IAP was in operation from 1995 to 2003 (e.g. [Esko et al., 1999](#)). For daylight operation a narrow band wavelength filter called FADOF (Faraday Anomalous Dispersion Optical Filter) was installed in the detection system ([Fricke-Begemann et al., 2002a](#)). Initial daytime measurements of densities and temperatures were carried out with the mobile K-lidar at Tenerife ( $28^\circ$  N) and Spitsbergen ( $78^\circ$  N) (e.g. [Lübben and Höffner, 2004](#)). This technology was also applied to the stationary K-lidar in Kühlungsborn which has been fully operational since February 2002. Both instruments are similar and operate with the same configuration. To minimize the contamination by solar background radiation the field of view (FOV) of the telescope and the laser beam divergence is reduced to  $186 \mu\text{rad}$  and  $133 \mu\text{rad}$ , respectively. A small laser beam divergence potentially causes saturation effects, i.e. the backscattered signal is no longer proportional to the laser power ([von der Gathen, 1991](#)). We have determined the effect of saturation on the potassium density measurements by switching between various fields of view and

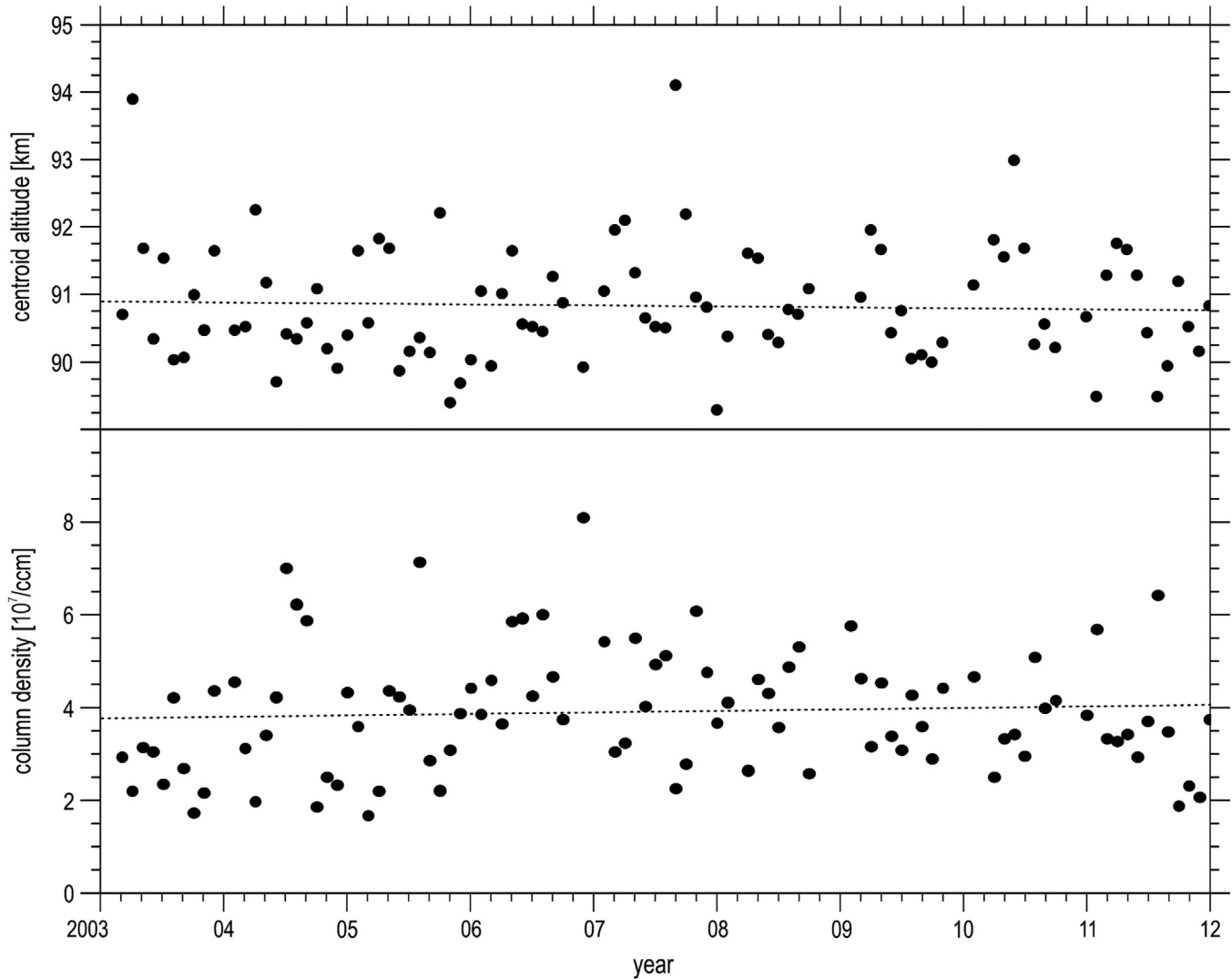


**Fig. 7.** Monthly mean of: Top: centroid altitude; Bottom: column density, with linear fit (dashed lines). Night time observations only, year 2003–2012.

beam divergence during night, i.e., when solar background is not a problem (Fricke-Begemann, 2004). On the basis of these measurements we have increased the densities by a factor of 3 for all data. The same correction factor was independently determined by Höffner and Lübken (2007) for the mobile K-lidar which has a similar configuration than the stationary K-lidar in Kühlungsborn. The uncertainty in this correction factor is approximately 30% but the factor itself is constant over time. All measurements regardless of day or night have been performed with the same setup e.g. FOV, laser beam divergence, daylight filter, optical pathways counting electronics etc. The configuration of the system was unchanged over the years besides the unavoidable replacement of flash lamps of the pulsed laser once or twice per year. In particular all critical parameter such as FOV, laser divergence, pulse energy were kept practically constant.

### 3. Observations and data analysis

Regular potassium density measurements were made with the stationary K-lidar over Kühlungsborn, Germany ( $54.1^{\circ}$  N,  $11.7^{\circ}$  E) starting February 15, 2002 and ending February 25, 2012. The 10-year data base consists of a total of 5090 h on 741 days. The time-of-day coverage of every profile ( $\sim 2$  min) is shown in Fig. 1. The gray shaded area indicates a solar elevation of  $0^{\circ}$  or less. The total data set includes 74.8% of night time measurements and 25.2% of daylight measurements.

Individual profiles are taken approximately every two minutes. After calculating the potassium densities from the individual profiles, all available profiles within a certain time frame or a whole day are averaged to obtain mean values with an altitude resolution of 200 m. To investigate the main potassium layer a lower limit of 2 atoms/cc is applied (Section 4). Much lower number densities can be detected at darkness by the K-lidar depending on the temporal resolution. During darkness the sensitivity of the K-lidar can be as low as 0.01 atoms/cc (Höffner and Friedman, 2005). However, despite the less favourable daytime observing conditions (i.e. due to the associated high solar background), it is still possible to achieve a minimum detection limit of 0.25 atoms/cc.

### 4. Properties of the potassium layer

An example for the daily course of the potassium number density is shown in Fig. 2. Densities larger than 2 atoms/cc are shown on a 2 min time and 200 m altitude grid without any further data processing except background subtraction. During sunrise, the background already starts to rise even if the Sun is a few degrees below the horizon. As a consequence all measurements at day suffer from noise. Nevertheless, it is still possible to observe the potassium layer with high resolution throughout the day. Note that a sporadic layer appearing at an altitude of 115 km and slowly declining over 12 h is visible at day and night time. Similar features occasionally occur from April to August and more frequently during June and July. However they are beyond the scope of this paper and

a follow-up paper will thoroughly investigate those layers.

To present the seasonal variation of the main potassium layer of the 10-year data set, the average density of each day and altitude (200 m) has been calculated. Then all measurements are interpolated with a 2-dimensional Hanning filter with a resolution of 1 km and 21 days. In contrast to the often performed annual and semi-annual fit no prior model of the seasonal variation is assumed. Fig. 3 shows the seasonal variation of the main potassium layer. Table 1 contains the average potassium layer of the whole data set with the lowest limit possible, 0.25 atoms/cc. The observable lower and upper boundaries of the potassium layer depends on the sensitivity of the instrument. In particular with such a low limit the topside at approximately 120 km altitude becomes visible and the lower boundary of the layer is as low as 77 km in winter time (Höffner and Friedman, 2005).

Since the variability of the layer on time scales of hours or days is large, a temporal smoothing with a 21-day Hanning filter was applied (see above). Even though the same lower limit of Fig. 2 is applied, no signs of sporadic layers are visible any more. Sporadic layers, meteor trails and other seldom occurring events of short duration have a minor impact on the main layer. We have therefore not removed such events from our data set.

Figs. 4–6 show the centroid height, column density and peak density of the potassium layer, respectively. The potassium layer is permanently present between 83 km and 98 km with a lower limit of 2 atoms/cc. In contrast to other metal species like sodium or iron, a clear semi-annual variation is visible (e.g. She et al., 2000; Gerding et al., 2000; Yuan et al., 2012). Both the column density and the peak density are higher at solstices compared to equinox (Figs. 5 and 6). The peak number density has two broad maxima: the first maximum occurs in summer and lasts for about 4 months (May–August) with number densities up to 60 atoms/cc. The second maximum is observed from early December to late February with densities up to 30 atoms/cc. Both maxima appear with some substructural local maxima which occur every year.

The variability of the column density and layer altitude is shown in Fig. 7. The average column density for all measurements of a given month was calculated. The data was limited to night time observations to avoid unequal sampling throughout the day and a possible bias by tides. The variability in column density and layer altitude is partly caused by the variation of the layer within a particular season. Over this whole period a weak positive trend of only 8% in the column density can be determined from a linear fit. We cannot rule out that this very small trend is caused by saturation as discussed before. However saturation does not influence the determination of the altitude of the layer which shows a small downward trend of approximately 130 m over 10 years. Even though it is not clear without further analysis if the observed trend is real, we can conclude that the layer shows very little long term changes over this 10-year period. A follow-up paper will use a whole-atmosphere climate model to investigate whether these changes in the observed potassium layer presented here are related to the 11-year solar cycle.

**Table 1**

Climatology of potassium density between 77 and 120 km at Kühlungsborn 54° N; densities lower than 0.25 atoms/cc are not shown.

Altitude	Day of year (every first and 15th of the month)																									
	1	15	32	46	60	74	91	105	121	135	152	166	182	196	213	227	244	258	274	288	305	319	335	349		
120												0.43	0.47	0.26												
119												0.59	0.47	0.30												
118												0.85	0.41	0.26												
117												0.87	0.33	0.25	0.26											
116												0.26	0.78	0.35	0.30	0.37										
115												0.28	0.73	0.42	0.38	0.52										
114												0.32	0.73	0.34	0.44	0.68	0.27					0.28	0.28			
113												0.38	0.93	0.27	0.45	0.83	0.35					0.31	0.34			
112												0.43	1.13	0.30	0.48	0.99	0.43					0.36	0.41	0.25		
111	0.26											0.46	1.16	0.42	0.52	1.15	0.52	0.25					0.39	0.46	0.31	0.30
110	0.27	0.34										0.47	1.02	0.47	0.55	1.25	0.62	0.37					0.41	0.50	0.38	0.38
109	0.33	0.40	0.32	0.28				0.26				0.49	0.97	0.47	0.56	1.27	0.71	0.53					0.41	0.56	0.47	0.47
108	0.43	0.53	0.43	0.37	0.26			0.30				0.50	0.96	0.53	0.56	1.19	0.74	0.65					0.31	0.34	0.59	0.57
107	0.59	0.78	0.59	0.50	0.36	0.29	0.37					0.50	0.70	0.46	0.49	1.02	0.76	0.78	0.29	0.30	0.28	0.33	0.45	0.68	0.73	0.72
106	0.80	1.03	0.80	0.70	0.50	0.40	0.46	0.29	0.27	0.48	0.26		0.43	0.84	0.80	0.91	0.38	0.41	0.40	0.45	0.60	0.84	0.93	0.94		
105	1.09	1.33	1.10	0.98	0.69	0.55	0.56	0.38	0.35	0.48	0.37	0.27	0.44	0.71	0.86	0.98	0.47	0.56	0.58	0.62	0.83	1.09	1.21	1.26		
104	1.52	1.74	1.53	1.42	1.00	0.79	0.72	0.55	0.48	0.52	0.65	0.57	0.48	0.70	0.95	0.96	0.59	0.77	0.82	0.86	1.17	1.45	1.64	1.74		
103	2.13	2.31	2.17	2.09	1.45	1.16	1.03	0.83	0.72	0.65	0.79	0.66	0.54	0.80	1.12	0.98	0.79	1.07	1.13	1.18	1.66	1.98	2.29	2.46		
102	2.94	3.08	3.09	3.02	2.09	1.73	1.53	1.35	1.17	0.95	0.86	0.66	0.58	0.98	1.41	1.22	1.12	1.49	1.54	1.64	2.36	2.69	3.22	3.47		
101	4.10	4.20	4.40	4.21	2.94	2.58	2.33	2.29	2.01	1.56	1.09	0.68	0.66	1.25	1.87	1.76	1.62	2.10	2.09	2.26	3.30	3.62	4.42	4.79		
100	5.69	5.73	6.15	5.77	4.13	3.81	3.59	3.90	3.57	2.83	1.69	0.86	0.88	1.74	2.64	2.60	2.40	3.02	2.89	3.12	4.53	4.82	5.86	6.40		
99	7.66	7.62	8.33	7.83	5.77	5.61	5.48	6.41	6.34	5.39	2.71	1.35	1.31	2.49	3.82	3.82	3.56	4.46	4.10	4.27	6.05	6.30	7.53	8.32		
98	9.86	9.71	10.9	10.5	7.90	8.19	7.99	9.76	10.6	10.1	4.28	2.26	2.10	3.57	5.38	5.49	5.33	6.56	5.80	5.78	7.89	8.04	9.47	10.5		
97	12.3	12.0	14.0	13.7	10.4	11.6	10.9	13.8	16.1	17.0	6.87	3.83	3.48	5.21	7.44	7.97	8.11	9.21	7.98	7.63	10.0	10.1	11.8	12.9		
96	14.9	14.7	17.7	17.6	13.3	15.2	14.0	18.4	22.7	25.1	11.1	6.73	6.12	8.13	10.7	11.9	12.5	12.2	10.5	9.80	12.3	12.6	14.6	15.4		
95	17.7	17.5	22.0	21.9	16.4	18.5	16.8	22.9	29.6	32.8	17.8	11.9	11.1	13.5	16.1	17.8	19.1	15.5	13.4	12.3	14.5	15.5	18.1	18.2		
94	20.1	20.2	26.1	26.1	19.7	21.0	18.9	26.3	35.7	40.5	27.3	20.0	19.2	22.1	24.0	25.7	27.4	18.9	16.3	15.0	17.0	18.5	21.6	21.0		
93	22.4	22.8	29.3	29.3	22.9	22.8	19.9	27.8	40.1	48.1	38.0	30.3	30.0	33.0	34.1	35.3	35.4	22.0	18.8	17.4	19.7	20.8	24.6	23.8		
92	24.7	25.3	31.2	31.1	25.3	23.6	20.0	27.9	42.0	53.5	48.0	41.0	40.5	42.9	44.5	45.1	40.7	24.3	20.4	19.1	22.3	22.2	26.7	26.2		
91	27.0	27.7	32.0	31.6	26.5	23.5	19.4	26.6	41.1	54.7	55.1	48.9	47.3	49.4	53.3	53.1	42.7	25.4	20.9	19.6	24.0	23.1	28.0			
90	29.0	29.5	31.6	31.1	26.4	22.5	18.2	24.3	37.3	51.4	56.9	51.7	48.9	52.2	58.8	57.7	43.0	25.4	20.4	19.2	25.1	23.9	28.7	29.2		
89	29.9	30.4	30.4	29.7	25.0	20.6	16.7	21.5	32.0	44.7	53.0	49.8	45.5	50.4	59.6	57.8	42.4	24.5	19.2	18.4	25.5	24.2	28.6	29.8		
88	29.2	30.0	28.5	27.5	22.8	17.9	15.0	18.3	26.1	36.0	44.6	44.0	38.5	43.9	55.1	53.0	40.3	22.8	17.6	17.4	24.9	23.3	26.9	29.3		
87	26.9	28.4	26.0	24.8	20.1	14.9	13.0	14.9	20.2	26.6	33.4	35.0	29.3	34.0	45.8	44.8	36.4	20.5	15.5	15.8	23.0	21.4	23.9	27.5		
86	23.2	25.7	22.8	21.6	17.2	11.7	10.7	11.3	14.5	17.9	21.7	23.7	19.4	23.1	34.0	34.9	30.9	17.6	13.2	13.7	20.1	19.4	20.8			
85	18.3	21.9	18.7	17.8	14.1	8.75	8.15	7.96	9.22	10.9	12.2	13.5	10.7	13.6	22.4	24.5	23.7	14.0	10.8	11.3	17.1	17.5	17.7	21.1		
84	13.0	17.6	14.2	13.9	10.9	5.99	5.58	5.05	5.03	5.63	5.77	6.36	4.84	6.96	13.1	15.0	15.5	9.85	8.12	8.75	14.2	15.3	14.2	16.8		
83	8.33	13.2	10.1	10.5	7.75	3.60	3.30	2.73	2.31	2.29	2.09	2.26	1.75	3.09	6.68	7.59	8.23	5.80	5.42	6.07	11.2	12.4	10.3	12.0		
82	4.77	8.80	6.74	7.56	5.01	1.84	1.66	1.18	0.87	0.70	0.31	0.40	1.09	2.93	2.98	3.40	2.76	3.09	3.61	7.83	8.95	6.58	8.03			
81	2.50	5.06	4.22	4.96	2.85	0.79	0.69	0.36	0.25					1.01	0.80	1.03	1.02	1.47	1.81	4.76	5.52	3.69	5.40			
80	1.19	2.47	2.45	2.77	1.39	0.27											0.57	0.77	2.53	3.01	1.92	3.84				
79	0.51	1.03	1.32	1.28	0.56													0.29	1.21	1.54	0.99	2.59				
78	0.41	0.68	0.49																	0.53	0.73	0.49	1.40			
77																				0.32	0.52					

## 5. Summary

Observations of potassium densities were performed in the mesopause region at Kühlungsborn, 54° N over the years 2002–2012. The 10-year diurnal data set comprises 5090 h at 741 days of which, 25.2% (1282 h) of all measurements were made during daytime. This comprehensive data set shows only little variation of the potassium layer over the years. Potassium number densities show a clear semi-annual variation with two broad maxima reoccurring every year. The first maximum occurs in summer and lasts for about 4 months (May–August) with number densities of up to 60 atoms/cc. The second maximum is observed from early December to late February with densities of up to 30 atoms/cc.

## Acknowledgments

Numerous students and colleagues were involved in the data collection over the years. The authors thank Cord Fricke-Begemann who assisted in performing measurements, technical innovations and data processing in the earlier years of observations. The measurements and the smooth operation of the K-lidar were further supported by our colleagues T. Köpnick and M. Priester. The data for this paper are curated by the Leibniz Institute of Atmospheric Physics, Kühlungsborn, Germany.

The Arecibo Observatory is operated by SRI International under a cooperative agreement with the National Science Foundation (AST-1100968), and in alliance with Ana G. Méndez-Universidad Metropolitana, and the Universities Space Research Association (USRA).

## References

- Alpers, M., Höffner, J., von Zahn, U., 1990. Iron atom densities in the polar mesosphere from lidar observations. *Geophys. Res. Lett.* 17, 2345–2348.
- Dawkins, E.C.M., Plane, J.M.C., Chipperfield, M.P., Feng, W., Gumbel, J., Hedin, J., Höffner, J., Friedman, J.S., 2014. First global observations of the mesospheric potassium layer. *Geophys. Res. Lett.* 41, 5653–5661.
- Esko, V., Höffner, J., von Zahn, U., 1998. Upper atmosphere potassium layer and its seasonal variations at 54° N. *J. Geophys. Res.* 103, 29207–29214.
- Esko, V., von Zahn, U., Plane, J.M.C., 1999. The terrestrial potassium layer (75–110 km) between 71° S and 54° N: observations and modeling. *J. Geophys. Res.* 104, 17173–17186.
- Felix, F., Keenliside, W., Kent, G., Sandford, M., 1973. Laser radar observations of atmospheric potassium. *Nature* 246, 345–346.
- Feng, W., Höffner, J., Marsh, D.R., Chipperfield, M.P., Dawkins, E.C.M., Viehl, T.P., Plane, J.M.C., 2015. Diurnal variation of the potassium layer in the upper atmosphere. *Geophys. Res. Lett.* 42.
- Fricke, K., von Zahn, U., 1985. Mesopause temperatures derived from probing the hyperfine structure of the d2 resonance line of sodium by lidar. *J. Atmos. Terr. Phys.* 47, 499–512.
- Fricke-Begemann, C., 2004. Lidar Investigations of the Mesopause Region: Temperature Structure and Variability PhD dissertation. Leibniz-Institute of Atmospheric Physics e.V. at the University Rostock, ISSN 1615–8083.
- Fricke-Begemann, C., Alpers, M., Höffner, J., 2002a. Daylight rejection with a new receiver for potassium resonance temperature lidars. *Opt. Lett.* 27, 1932–1934.
- Fricke-Begemann, C., Höffner, J., von Zahn, U., 2002b. The potassium density and temperature structure in the mesopause region (80–105 km) at a low latitude (28° N). *Geophys. Res. Lett.* 29.
- Friedman, J.S., Collins, S.C., Delgado, R., Castleberg, P.A., 2002. Mesospheric potassium layer over the Arecibo observatory, 18.3° N 66.75° W. *Geophys. Res. Lett.* 29.
- Gerding, M., Alpers, M., von Zahn, U., Rollason, R.J., Plane, J.M.C., 2000. Atmospheric Ca and Ca+ layers: midlatitude observations and modeling. *J. Geophys. Res. Space Phys.* 105, 27131–27146.
- Höffner, J., Friedman, J., 2005. The mesospheric metal layer topside: examples of simultaneous metal observations. *J. Atmos. Solar-Terr. Phys.* 67, 1226–1237.
- Höffner, J., Lübken, F.-J., 2007. Potassium lidar temperatures and densities in the mesopause region at Spitsbergen (78° N). *J. Geophys. Res. Atmos.* 112.
- Höffner, J., von Zahn, U., 1995. Mesopause temperature profiling by potassium lidar: recent progress and outlook for ALOMAR. In: Blix, T.A. (Ed.), European Rocket and Balloon Programmes and Related Research, p. 403.
- Kopp, M., Gerding, M., Höffner, J., Lübken, F.-J., 2015. Tidal signatures in temperatures derived from daylight lidar soundings above Kühlungsborn (54° N, 12° E). *J. Atmos. Solar-Terrestrial Phys.* 127, 37–50.
- Llewellyn, E., Lloyd, N.D., Degenstein, D.A., Gatttinger, R.L., Petelina, S.V., Bourassa, A.E., Wiensz, J.T., Ivanov, E.V., McDade, I.C., Solheim, B.H., McConnell, J.C., Haley, C.S., von Savigny, C., Sioris, C.E., McLinden, C.A., Griffioen, E., Kaminski, J., Evans, W.F.J., Puckrin, E., Strong, K., Wehrle, V., Hum, R.H., Kendall, D.J.W., Matsushita, J., Murtagh, D.P., Brohede, S., Stegman, J., Witt, G., Barnes, G., Payne, W.F., Piché, L., Smith, K., Warshaw, G., Deslauniers, D.L., Marchand, P., Richardson, E.H., King, R.A., Wevers, I., McCreath, W., Kyrölä, E., Oikarinen, L., Leppelmeier, G.W., Auvinen, H., Megie, G., Hauchecorne, A., Lefevre, F., de La Nöe, J., Ricaud, P., Frisk, U., Sjoberg, F., von Schéele, F., Nordh, L., 2004. The OSIRIS instrument on the Odin spacecraft. *Can. J. Phys.* 82, 411–422.
- Lübken, F.-J., Höffner, J., 2004. Experimental evidence for ice particle interaction with metal atoms at the high latitude summer mesopause region. *Geophys. Res. Lett.* 31.
- Papen, G.C., Gardner, C.S., Pfenninger, W.M., 1995. Analysis of a potassium lidar system for upper-atmospheric wind-temperature measurements. *Appl. Opt.* 34, 6950–6958.
- Plane, J.M.C., Feng, W., Dawkins, E.C.M., Chipperfield, M., Höffner, J., Janches, D., Marsh, D., 2014. Resolving the strange behavior of extraterrestrial potassium in the upper atmosphere. *Geophys. Res. Lett.* 41, 4753–4760.
- She, C.Y., Chen, S., Hu, Z., Sherman, J., Vance, J., Vasoli, V., White, M., Yu, J., Krueger, D.A., 2000. Eight-year climatology of nocturnal temperature and sodium density in the mesopause region (80 to 105 km) over Fort Collins, Colorado (41° N, 105° W). *Geophys. Res. Lett.* 27, 3289–3292.
- Slipher, V., 1929. Emissions of the spectrum of the night sky. *Pop. Astron.* 37, 327.
- Sullivan, H.M., Hunten, D.M., 1962. Relative abundance of lithium, sodium and potassium in the upper atmosphere. *Lett. Nat.* 195, 589–590.
- von der Gathen, P., 1991. Saturation effects in Na lidar temperature measurements. *J. Geophys. Res. Atmos.* 96, 3679–3690.
- von Zahn, U., Höffner, J., 1996. Mesopause temperature profiling by potassium lidar. *Geophys. Res. Lett.* 23, 141–144.
- Yuan, T., She, C.Y., Kawahara, T.D., Krueger, D.A., 2012. Seasonal variations of mid-latitude mesospheric na layer and their tidal period perturbations based on full diurnal cycle na lidar observations of 20022008. *J. Geophys. Res. Atmos.* 117, n/a–D11304.